
000 SVD PROVABLY DENOISES NEAREST NEIGHBOR 001 002 DATA 003 004

005 **Anonymous authors**

006 Paper under double-blind review

007 008 ABSTRACT 009 010

011 We study the Nearest Neighbor Search (NNS) problem in a high-dimensional set-
012 ting where data originates from a low-dimensional subspace and is corrupted by
013 Gaussian noise. Specifically, we consider a semi-random model where n points
014 from an unknown k -dimensional subspace of \mathbb{R}^d ($k \ll d$) are perturbed by zero-
015 mean d -dimensional Gaussian noise with variance σ^2 on each coordinate. Without
016 loss of generality, we may assume the nearest neighbor is at distance 1 from the
017 query, and that all other points are at distance at least $1 + \varepsilon$. We assume we are
018 given only the noisy data and are required to find NN of the uncorrupted data. We
019 prove the following results:

020 1. For $\sigma \in O(1/k^{1/4})$, we show that simply performing SVD denoises the
021 data; namely, we provably recover accurate NN of uncorrupted data (Theo-
022 rem 1.1).
023 2. For $\sigma \gg 1/k^{1/4}$, NN in uncorrupted data is not even **identifiable** from the
024 noisy data in general. This is a matching lower bound on σ with the above
025 result, demonstrating the necessity of this threshold for NNS (Lemma 3.1).
026 3. For $\sigma \gg 1/\sqrt{k}$, the noise magnitude $(\sigma\sqrt{d})$ significantly exceeds the inter-
027 point distances in the unperturbed data. Moreover, NN in noisy data is dif-
028 ferent from NN in the uncorrupted data in general.

029 Note that (1) and (3) together imply SVD identifies correct NN in uncorrupted
030 data even in a regime where it is different from NN in noisy data. This was not the
031 case in existing literature (see e.g. (Abdullah et al., 2014)). Another comparison
032 with (Abdullah et al., 2014) is that it requires σ to be at least an inverse poly-
033 nomial in the ambient dimension d . The proof of (1) above uses upper bounds on
034 perturbations of singular spaces of matrices as well as concentration and spherical
035 symmetry of Gaussians. We thus give theoretical justification for the performance
036 of spectral methods in practice. We also provide empirical results on real datasets
037 to corroborate our findings.

038 039 1 INTRODUCTION 040

041 The nearest neighbor problem is a fundamental task in various fields, including machine learning,
042 data mining, and computer vision. It involves identifying the data point closest to a given query point
043 within a dataset. While conceptually straightforward, the performance and reliability of nearest
044 neighbor search (NNS) can suffer in the presence of noise, particularly in high-dimensional spaces.
045 Real-world data is susceptible to noise, which can ruin the true underlying structure and lead to
046 erroneous nearest neighbor identifications. This necessitates robust techniques that can reduce the
047 impact of noise to ensure accurate and reliable NNS. In this paper, we analyze the NNS problem in
048 a noisy high-dimensional setting. Specifically, we consider a semi-random model where data points
049 from an unknown k -dimensional subspace of \mathbb{R}^d ($k \ll d$) are perturbed by adding d -dimensional
050 Gaussian noise $N_d(0, \sigma^2 I_d)$ to it.

051 A fundamental tool in high-dimensional computational geometry, often applied to the NNS prob-
052 lem, is the random projection method. The Johnson-Lindenstrauss Lemma (Johnson and Linden-
053 strauss, 1984) demonstrates that projecting data onto a uniformly random k -dimensional subspace
054 of \mathbb{R}^d approximately preserves distances between points, offering a computationally efficient way

054 to reduce dimensionality. This approach has had a tremendous impact on algorithmic questions in
055 high-dimensional geometry, leading to the development of algorithms for approximate NNS, such
056 as Locality-Sensitive Hashing (LSH) (Indyk and Motwani, 1998), which are widely used both the-
057oretically and practically. All known variants of LSH for Euclidean space, including (Datar et al.,
058 2004; Andoni and Indyk, 2006; Andoni et al., 2014), involve random projections.

059 However, it is natural to question whether performance can be improved by replacing "random" pro-
060 jections with "best" or data-aware projections. Practitioners often rely on techniques like Principal
061 Component Analysis (PCA) and its variants for dimension reduction, leading to successful heuris-
062 tics such as PCA trees (McNames, 2001; Sproull, 1991; Verma et al., 2009), spectral hashing (Weiss
063 et al., 2008), and semantic hashing (Salakhutdinov and Hinton, 2009). These data-adaptive methods
064 frequently outperform algorithms based on oblivious random projections in practice. Yet, unlike ran-
065 dom projection methods, these adaptive approaches often lack rigorous correctness or performance
066 guarantees. Bridging this gap between theoretical guarantees and empirical successes for data-aware
067 projections is a significant open question in Massive Data Analysis, see, e.g., (Council, 2013). For
068 worst-case inputs, random projections are known to be theoretically optimal (Alon, 2003; Jayram
069 and Woodruff, 2013), making it challenging to theoretically justify data-aware improvements. This
070 paper aims to provide a theoretical justification for this disparity by studying data-aware projections
071 for the NNS problem.

072 To address this challenge, we study the semi-random setting proposed in (Abdullah et al., 2014).
073 In this setting, a dataset P of n points in \mathbb{R}^d , and a query point q are arbitrarily drawn from an
074 unknown k -dimensional subspace (where $k \ll d$) and then perturbed by adding d -dimensional
075 Gaussian noise $N_d(0, \sigma^2 I_d)$. The goal is to find the point $p \in P$ that is closest to q in Euclidean
076 distance (considering their unperturbed versions), based on noisy versions.

077 Our main contribution is a new Singular Value Decomposition (SVD) algorithm for solving the NNS
078 recovery problem. This algorithm can tolerate substantially larger noise levels compared to previous
079 approaches, such as those in (Abdullah et al., 2014). Specifically, we characterize the robustness
080 of NNS under various noise levels. We identify several critical noise level thresholds below in the
081 increasing order of noise level:

- 082 • For $\sigma \gg 1/\sqrt{d}$, the noise magnitude (with an expected magnitude of $\sigma\sqrt{d}$) can be sub-
083 stantially larger than the inter-point distances in the original data. Specifically, random
084 Johnson-Lindenstrauss projections will preserve these noisy distances, effectively losing
085 the underlying nearest neighbor structure of the uncorrupted data. Therefore, SVD would
086 be preferred to random projection when $\sigma \gg 1/\sqrt{d}$.
- 087 • For $\sigma \in O(1/d^{1/4})$, (Abdullah et al., 2014) proved that the nearest neighbor in the
088 perturbed data remains the same. Their algorithm tolerates a noise level of at most
089 $\sigma = O(1/\sqrt{kd}^{1/4})$, which implies σ must be at least an inverse polynomial in the am-
090 bient dimension d .
- 091 • For $\sigma \gg 1/\sqrt{k}$, the nearest neighbor in the perturbed data can, with large probability, differ
092 from the true nearest neighbor.
- 093 • For $\sigma \in O(1/k^{1/4})$, our algorithmic results (Theorem 1.1) demonstrate that applying SVD
094 to the perturbed data can effectively identify the true nearest neighbor in this regime. This
095 represents a critical improvement over the previous work of (Abdullah et al., 2014), as our
096 algorithm is effective for $\sigma \gg 1/\sqrt{k}$ where the NN in noisy data is different from the NN
097 in uncorrupted data.
- 098 • For $\sigma \gg 1/k^{1/4}$, we show that it is information-theoretically impossible to identify the
099 nearest neighbors from the noisy data. This result complements our algorithmic findings by
100 providing matching lower bounds on the noise level σ , thereby demonstrating the necessity
101 of the threshold $\sigma = O(1/k^{1/4})$ for NNS.

102 **1.1 HIGH-LEVEL OVERVIEW**

103 In addition to improved noise tolerance, our algorithm offers simplicity, requiring only two SVD
104 calls, unlike the iterated PCA approach in (Abdullah et al., 2014). We now discuss the high-level
105 idea of our algorithm. We represent the input points as the first n columns of a $d \times (n + 1)$ matrix

108 B , with the last column being the query point q . Similarly, we represent the Gaussian noise as a
109 $d \times (n+1)$ matrix C with i.i.d. entries drawn from $N(0, \sigma^2)$. Let $A = B + C$ denote the perturbed
110 data set, which serves as the input to our algorithm. Our approach involves computing the SVD of
111 A and projecting A onto its top k -dimensional subspace. A direct application of the SVD was not
112 explored in earlier works to handle such high noise levels. The only earlier work we are aware of
113 with related provable guarantees in a noisy model via the SVD is that on latent semantic indexing
114 (Papadimitriou et al., 2000), though (Papadimitriou et al., 2000) makes strong assumptions.

115 More specifically, we process the j indices in two parts: first for $1 \leq j \leq \frac{n}{2}$, then for $\frac{n}{2} + 1 \leq j \leq n$.
116 Let $A^{(1)}$ be a $d \times (\frac{n}{2} + 1)$ matrix consisting of the first $n/2$ columns of A and the query point (as
117 column $n/2 + 1$). Similarly, let $A^{(2)}$ be a $d \times (\frac{n}{2} + 1)$ matrix formed by the last $n/2$ columns of
118 A and the query point. The query point is in both parts. This superscript notation, (1) and (2), is
119 also extended to B and C . Let $U^{(1)}$ be the subspace spanned by the k top singular vectors of the
120 first $n/2$ columns of $A^{(1)}$ (i.e., $A^{(1)}[1, \frac{n}{2}]$). Similarly, $U^{(2)}$ is the subspace spanned by the k top
121 singular vectors of the first $n/2$ columns of $A^{(2)}$ (i.e., $A^{(2)}[1, \frac{n}{2}]$). Since $A^{(1)}$ and $A^{(2)}$ are given,
122 $U^{(1)}$ and $U^{(2)}$ can be computed. The point of splitting the data into 2 parts is that $P_{U^{(2)}}$ and $A^{(1)}$ are
123 stochastically independent and this makes our probabilistic arguments simpler. It is not clear that
124 this is necessary and we leave it as an open question as to whether the simpler algorithm without
125 splitting provably works.
126

127 We denote the projection matrix onto a subspace $U \subseteq \mathbb{R}^d$ as P_U . The underlying idea is that pro-
128 jecting points (both data and query) onto the SVD subspace effectively extracts the latent subspace
129 structure, which is sufficient to estimate distances, $\|p_i - q\|$. Thus, the main algorithm proceeds as
130 follows: to estimate all distances for the first $n/2$ points, we compute the minimum value of:

$$131 \min_{1 \leq j \leq \frac{n}{2}} \left\| P_{U^{(2)}} \left(A_{\cdot, j}^{(1)} - A_{\cdot, n/2+1}^{(1)} \right) \right\|,$$

133 where $A_{\cdot, j}^{(1)}$ denotes the j -th column of $A^{(1)}$. With $x_j = \mathbf{e}_j - \mathbf{e}_{n/2+1}$, this expression simplifies
134 to $\|P_{U^{(2)}} A^{(1)} x_j\|$. Our claim is that, under a specific noise regime, $\|P_{U^{(2)}} A^{(1)} x_j\|$ provides a
135 $(1 + \varepsilon)$ -approximation of $\|B^{(1)} x_j\| = \|p_i - q\|$ for any $\varepsilon > 0$. Subsequently, similar steps are
136 performed for the second part of the data. The complete algorithm is then as follows:
137

138 **Algorithm 1** $(1 + \varepsilon)$ -approximate NNS for the Semi-Random Model

140 **Require:** An ambient space \mathbb{R}^d and a matrix $A \in \mathbb{R}^{d \times (n+1)}$ representing the perturbed point set.
141 **Ensure:** Returns the index of a $(1 + \varepsilon)$ -approximate nearest neighbor for the unperturbed data.

142 1: $A^{(1)} \leftarrow$ matrix formed by columns 1 to $n/2$ of A and column $n + 1$ of A .
143 2: $A^{(2)} \leftarrow$ matrix formed by columns $n/2 + 1$ to n of A and column $n + 1$ of A .
144 3: $U^{(1)} \leftarrow$ the subspace spanned by the k top singular vectors of $A^{(1)}$.
145 4: $U^{(2)} \leftarrow$ the subspace spanned by the k top singular vectors of $A^{(2)}$.
146 5: $j_1 \leftarrow \arg \min_{1 \leq j \leq \frac{n}{2}} \|P_{U^{(2)}} A^{(1)} x_j\|$.
147 6: $j_2 \leftarrow \arg \min_{1 \leq j \leq \frac{n}{2}} \|P_{U^{(1)}} A^{(2)} x_j\|$.
148 7: **if** $\|P_{U^{(2)}} A^{(1)} x_{j_1}\| < \|P_{U^{(1)}} A^{(2)} x_{j_2}\|$ **then**
149 8: Return j_1 .
150 9: **else**
151 10: Return $j_2 + n/2$.
152 11: **end if**

154 Below, we formalize the theoretical guarantee of Algorithm 1. Let $s_k(X)$ denote the k -th singular
155 value of matrix X . If $\text{rank}(X) < k$, then $s_k(X)$ is defined as 0.

156 **Theorem 1.1.** *For the semi-random model described above, if the noise level σ satisfies:*

$$158 \sigma \leq \min \left(\sqrt{\frac{\varepsilon}{240}} \frac{\min(\|B^{(1)} x_j\|, \|B^{(2)} x_j\|)}{(k \ln n)^{1/4}}, \frac{\varepsilon \cdot \min(s_k(B^{(1)}), s_k(B^{(2)}))}{75\sqrt{n}}, \frac{\varepsilon \cdot \min(\|B^{(1)} x_j\|, \|B^{(2)} x_j\|)}{36\sqrt{\ln n}} \right),$$

160 161 then Algorithm 1 returns a $(1 + \varepsilon)$ -approximate nearest point for any $\varepsilon > 0$ with probability at least
162 $1 - \frac{1}{n}$.

162 **Remark 1.2** (Interpretation of Bounds). *Theorem 1.1 highlights two distinct scaling requirements*
 163 *for recovery:*

164

- 165 1. **Intrinsic Dimension (k):** *The term $O(1/k^{1/4})$ reflects the geometric complexity of the*
 166 *subspace. This threshold aligns with the information-theoretic limits of preserving nearest*
 167 *neighbor structures (see Lemma 3.1).*
- 168 2. **Signal Strength ($s_k(B)$):** *The term proportional to $s_k(B)/\sqrt{n}$ bounds the spectral gap.*
 169 *By Wedin’s Theorem, this ratio ensures that the principal angles between the true subspace*
 170 *V and the empirical subspace $U^{(2)}$ remain small. If $s_k(B)$ were too small, the signal*
 171 *directions would be indistinguishable from noise directions, making subspace recovery im-*
 172 *possible regardless of the algorithm used. We discuss this factor in Section 2.3.*

173 This highlights the power of SVD in extracting low-dimensional structure from noisy high-
 174 dimensional observations. We also explored its impact through our empirical results. Our empirical
 175 results further validate our theoretical findings, demonstrating the practical benefits of our SVD-
 176 based approach and its superior performance compared to naive algorithms, particularly in terms
 177 of noise dependence on the intrinsic subspace dimension k and sensitivity to the k -th minimum
 178 singular value of the data $s_k(B)$.

179 **Organization:** Section 2 details our algorithmic approach, including the problem setup and the
 180 SVD-based algorithm, along with its analysis and discussion. Section 3 provides theoretical lower
 181 bounds, demonstrating the optimality of our proposed noise thresholds. Finally, Section 4 presents
 182 empirical results that validate our theoretical findings and illustrate the practical benefits of our
 183 approach.

185 **2 ALGORITHMIC RESULTS**

186 **2.1 THE MODEL AND PROBLEM**

187 We employ a semi-random data model that assumes the original data consists of n arbitrary (not
 188 random) points from a k -dimensional subspace V of \mathbb{R}^d . We also assume the query point lie in
 189 V . The original data is latent (hidden), and so is V . The input is noisy data, obtained by adding
 190 Gaussian noise to the original data. Such a semi-random model has been widely used (Abdullah
 191 et al., 2014; Azar et al., 2001).

192 B is a $d \times (n + 1)$ matrix where the first n columns represent the latent data points, and the last
 193 column represents the latent query. C is a $d \times (n + 1)$ matrix representing the perturbations to the
 194 n latent data points and the query. We assume the entries of C are i.i.d. random variables, each
 195 drawn from $N(0, \sigma^2)$. The observed data $A = B + C$ constitutes the input to the problem. For
 196 notational convenience, let $x'_j = \mathbf{e}_j - \mathbf{e}_{n+1}$ such that $B_{\cdot, j} - B_{\cdot, n+1} = Bx'_j$. The objective is to
 197 output a $(1 + \varepsilon)$ -approximate nearest neighbor for $\varepsilon > 0$. Specifically, the goal is to find an index
 198 $j \in \{1, 2, \dots, n\}$ satisfying $\|Bx'_j\| \leq (1 + \varepsilon) \cdot \min_{1 \leq i \leq n} \|Bx'_i\|$.

202 **2.2 ANALYSIS**

203 We are now ready to start the proof of Theorem 1.1. We said that $\|P_{U^{(2)}} A^{(1)} x_j\|$ is a good ap-
 204 proximation to $\|B^{(1)} x_j\|$. Below, Lemma 2.1 quantifies how well the projected noisy distances
 205 approximate the true latent distances, plus an expected noise term $(2k\sigma^2)$. Hence, we can infer
 206 that if j satisfies: $\|P_{U^{(2)}} A^{(1)} x_j\| = \min_{1 \leq i \leq n/2} \|P_{U^{(2)}} A^{(1)} x_i\|$, then, j approximately minimizes
 207 $\|B^{(1)} x_j\|$ over $\|B^{(1)} x_i\|$ for $1 \leq i \leq n/2$ within error at most the right hand side of (1).

208 **Lemma 2.1.** *Assume $B^{(1)}$ has rank k , $n \geq d$, and $k \geq \ln n$. Then, for each $1 \leq j \leq n/2$, the*
 209 *following holds with at least $1 - \frac{1}{n^2}$ probability:*

$$\begin{aligned}
 & \left| \left\| P_{U^{(2)}} A^{(1)} x_j \right\|^2 - 2k\sigma^2 - \left\| B^{(1)} x_j \right\|^2 \right| \\
 & \leq \frac{100\sigma^2 n}{s_k^2(B^{(2)})} \left\| B^{(1)} x_j \right\|^2 + \frac{40\sigma\sqrt{n}}{s_k(B^{(2)})} \left\| B^{(1)} x_j \right\|^2 + 20\sigma \left\| B^{(1)} x_j \right\| \sqrt{\ln n} + 40\sigma^2 \sqrt{k \ln n}. \quad (1)
 \end{aligned}$$

216 Similarly, assuming $B^{(2)}$ has rank k , $n \geq d$, and $k \geq \ln n$, then for each $1 \leq j \leq n/2$, the following
217 holds with at least $1 - \frac{1}{n^2}$ probability:
218

$$219 \quad \left| \left\| P_{U^{(1)}} A^{(2)} x_j \right\|^2 - 2k\sigma^2 - \left\| B^{(2)} x_j \right\|^2 \right| \\ 220 \quad \leq \frac{100\sigma^2 n}{s_k^2(B^{(1)})} \left\| B^{(2)} x_j \right\|^2 + \frac{40\sigma\sqrt{n}}{s_k(B^{(1)})} \left\| B^{(2)} x_j \right\|^2 + 20\sigma \left\| B^{(2)} x_j \right\| \sqrt{\ln n} + 40\sigma^2 \sqrt{k \ln n}.$$

221
222
223
224

225 *Proof.* Without loss of generality, we prove only the first part. Since all data points and the query
226 point q lie in V , projecting $B^{(1)}$ onto V does not change it. Thus, $P_V B^{(1)} = B^{(1)}$. Therefore, the
227 following holds:

$$228 \quad P_{U^{(2)}} A^{(1)} = P_{U^{(2)}} (B^{(1)} + C^{(1)}) = B^{(1)} + (P_{U^{(2)}} - P_V) B^{(1)} + P_{U^{(2)}} C^{(1)}.$$

229

230 We aim to bound each term in this expression. First, $\|P_{U^{(2)}} - P_V\|$ can be bounded in terms of
231 the k -th singular value $s_k(B^{(1)})$. Second, $P_{U^{(2)}} C^{(1)} x_j$ is a random Gaussian vector, as per the
232 definition of the noise matrix C . Thus, in the lemma statement, terms containing $s_k(B^{(1)})$ relate to
233 the effect of the $(P_{U^{(2)}} - P_V) B^{(1)} x_j$ term, while the remaining terms are associated with the inner
234 product of random Gaussian noise or the norm of the noise vector itself.

235 Since $P_{U^{(2)}}$ is symmetric, we get:

$$236 \quad \left\| P_{U^{(2)}} A^{(1)} x_j \right\|^2 = \left\| B^{(1)} x_j + (P_{U^{(2)}} - P_V) B^{(1)} x_j + P_{U^{(2)}} C^{(1)} x_j \right\|^2 \\ 237 \quad = \left\| B^{(1)} x_j \right\|^2 + \left\| (P_{U^{(2)}} - P_V) B^{(1)} x_j \right\|^2 + \left\| P_{U^{(2)}} C^{(1)} x_j \right\|^2 \\ 238 \quad + 2x_j^T B^{(1)T} (P_{U^{(2)}} - P_V) B^{(1)} x_j + 2x_j^T B^{(1)T} P_{U^{(2)}} C^{(1)T} x_j + 2x_j^T C^{(1)T} P_{U^{(2)}} (P_{U^{(2)}} - P_V) B^{(1)} x_j. \\ 239 \quad (2)$$

240
241
242
243

244 Now, $P_{U^{(2)}}$ is idempotent: $P_{U^{(2)}} P_{U^{(2)}} = P_{U^{(2)}}$. Also since the columns of $B^{(1)}$ lie in V , we have
245 $P_V B^{(1)} = B^{(1)}$. Plugging these into the last term on the right hand side of (2), we see that term
246 is zero ($P_{U^{(2)}} (P_{U^{(2)}} - P_V B^{(1)}) = 0$). It turns out that each of the other terms can be bounded.
247 By Lemma 2.4, Lemma 2.5, Lemma 2.6, and Lemma 2.7 below, together with the union bound, the
248 theorem is proved. \square

249 Before proving the lemmas directly, we first show a bound on the spectral norm of the matrix $P_{U^{(2)}} -$
250 P_V . Recall that V is the true underlying subspace containing the points and the query, while $U^{(2)}$
251 is the subspace spanned by the columns of the perturbed matrix A . Thus, bounds on the spectral
252 norm of the difference between these two projection matrices can be expressed in terms of the noise
253 σ as follows. For this, we use well-established results from Numerical Analysis, namely, the $\sin \Theta$
254 theorem by (Davis and Kahan, 1970) and the corresponding theorem for singular subspaces due to
255 (Wedin, 1972), which is stated as Lemma 2.2 below:

256 **Lemma 2.2** ((O'Rourke et al., 2018, Theorem 19)). *Let B be a real $d \times n$ matrix with singular
257 values $s_1 \geq \dots \geq s_{\min(d,n)} \geq 0$ and corresponding singular vectors $v_1, \dots, v_{\min(d,n)}$. Also, let E
258 be an $d \times n$ perturbation matrix. Let $s'_1 \geq \dots \geq s'_{\min(d,n)} \geq 0$ denote the singular values of $B + E$
259 with corresponding singular vectors $v'_1, \dots, v'_{\min(d,n)}$. Suppose the rank of B is r . For $1 \leq j \leq r$,
260 let V_j and V'_j be the subspaces spanned by $\{v_1, \dots, v_j\}$ and $\{v'_1, \dots, v'_j\}$. Then, if V_j and V'_j are
261 both j dimensional spaces, the following holds for the (principal) angle between two subspaces:*

$$262 \quad \sin \angle(V_j, V'_j) := \max_{v \in V_j, v \neq 0} \min_{v' \in V'_j, v' \neq 0} \sin \angle(v, v') = \left\| P_{V_j} - P_{V'_j} \right\| \leq \frac{2\|E\|}{s_j - s_{j+1}}$$

263
264
265

266 where $s_{r+1} = 0$.

267

268 The bound in Lemma 2.2 is in terms of the $\|E\|$ term, which is the spectral norm of the perturbation
269 matrix. To use this, we need an upper bound on $\|E\|$. For this, we use a well-known result from
Random Matrix Theory:

270 **Lemma 2.3** ((Rudelson and Vershynin, 2010, Equation 2.3)). Suppose all entries of a $d \times n$ matrix
 271 E are sampled from $N(0, \sigma^2)$ i.i.d. Then the following holds for any $t \geq 0$:

$$273 \quad \Pr \left[\|E\| > \sigma(\sqrt{n} + \sqrt{d}) + t \right] \leq 2 \exp \left(- \frac{t^2}{2\sigma^2} \right).$$

275 **Lemma 2.4.** Assume that $n \geq d$, and $B^{(2)}$ has rank k . Then for all $1 \leq j \leq n/2$, the following
 276 holds with at least $1 - \frac{1}{4n^2}$ probability:

$$278 \quad \left\| (P_{U^{(2)}} - P_V) B^{(1)} x_j \right\|^2 \leq \frac{100\sigma^2 n}{s_k^2(B^{(2)})} \left\| B^{(1)} x_j \right\|^2.$$

280 **Lemma 2.5.** Assume $k \geq \ln n$ and $n \geq d$. Then $\left| \left\| P_{U^{(2)}} C^{(1)} x_j \right\|^2 - 2k\sigma^2 \right| \leq 40\sqrt{\ln n} \sqrt{k}\sigma^2$ holds
 281 for all $1 \leq j \leq n/2$, with at least $1 - \frac{1}{2n^2}$ probability.

283 **Lemma 2.6.** Assume $n \geq d$, and $B^{(2)}$ has rank k . Then, for all $1 \leq j \leq n/2$, the following holds
 284 with at least $1 - \frac{1}{2n^2}$ probability.:

$$286 \quad \left| x_j^T B^{(1)T} (P_{U^{(2)}} - P_V) B^{(1)} x_j \right| \leq \frac{4\sigma\sqrt{n}}{s_k(B^{(2)})} \left\| B^{(1)} x_j \right\|^2.$$

288 **Lemma 2.7.** For all $1 \leq j \leq n/2$, the following holds:

$$290 \quad \left| x_j^T B^{(1)T} P_{U^{(2)}} C x_j \right| \leq 3\sigma \left\| B^{(1)} x_j \right\| \sqrt{\ln n}$$

291 with at least $1 - \frac{1}{4n^2}$ probability.

293 We now use Lemma 2.1 to prove the following corollary, which quantifies the noise level tolerance
 294 needed for a $(1 \pm O(\varepsilon))$ -approximation of the distance:

295 **Corollary 2.8.** Suppose the noise σ satisfies:

$$296 \quad \sigma \leq \min \left(\sqrt{\frac{\varepsilon}{240}} \frac{\left\| B^{(1)} x_j \right\|}{(k \ln n)^{1/4}}, \frac{\varepsilon s_k(B^{(1)})}{75\sqrt{n}}, \frac{\varepsilon \left\| B^{(1)} x_j \right\|}{36\sqrt{\ln n}} \right).$$

299 Then, we have

$$300 \quad \left\| P_{U^{(2)}} A^{(1)} x_j \right\|^2 - 2k\sigma^2 \in \left[\left(1 - \frac{\varepsilon}{3}\right) \left\| B^{(1)} x_j \right\|^2, \left(1 + \frac{\varepsilon}{3}\right) \left\| B^{(1)} x_j \right\|^2 \right]$$

302 for all $1 \leq j \leq \frac{n}{2}$ with at least $1 - \frac{1}{2n}$ probability. Similarly, the above holds for $A^{(2)}$ and $B^{(2)}$.

304 We now provide the proof of Theorem 1.1, which offers the theoretical guarantee for our main
 305 algorithm:

307 *Proof.* Our algorithm returns the index j corresponding to the minimum value found across two
 308 parts of the minimization: $\min_{1 \leq j \leq n/2} \left\| P_{U^{(2)}} A^{(1)} x_j \right\|$ and $\min_{n/2+1 \leq j \leq n} \left\| P_{U^{(1)}} A^{(2)} x_{j-n/2} \right\|$.
 309 Without loss of generality, assume that the first column of B (corresponding to p_1) is the nearest
 310 neighbor to the query point q , and $\left\| B^{(1)} x_1 \right\| = 1$. The proof then needs to show that the algorithm
 311 selects an index j^* such that $\left\| B^{(1)} x_{j^*} \right\| \leq 1 + \varepsilon$.

312 Suppose our algorithm returns an index j^* from the first part of the minimization, where $1 \leq j^* \leq$
 313 $n/2$. By the algorithm's logic, this implies:

$$315 \quad \left\| P_{U^{(2)}} A^{(1)} x_{j^*} \right\|^2 - 2k\sigma^2 \leq \left\| P_{U^{(2)}} A^{(1)} x_1 \right\|^2 - 2k\sigma^2.$$

317 Since the noise level σ satisfies the conditions of Corollary 2.8, we have:

$$318 \quad \left(1 - \frac{\varepsilon}{3}\right) \left\| B^{(1)} x_{j^*} \right\|^2 \leq \left\| P_{U^{(2)}} A^{(1)} x_{j^*} \right\|^2 \leq \left\| P_{U^{(2)}} A^{(1)} x_1 \right\|^2 \leq \left(1 + \frac{\varepsilon}{3}\right) \left\| B^{(1)} x_1 \right\|^2$$

320 This implies

$$321 \quad \left\| B^{(1)} x_{j^*} \right\|^2 \leq \frac{1 + \varepsilon/3}{1 - \varepsilon/3} \left\| B^{(1)} x_1 \right\|^2 \leq (1 + \varepsilon) \left\| B^{(1)} x_1 \right\|^2.$$

323 Thus, the desired result is obtained. If our algorithm returns an index j^* from the second part of the
 324 minimization, a similar argument establishes the correctness of our algorithm. \square

324 2.3 DISCUSSION
325

326 Our work shows recovery even when the noisy nearest neighbor has changed, whereas (Abdullah
327 et al., 2014) operates in a regime where the NN is preserved despite the noise, which is a key
328 conceptual distinction. However, Theorem 1.1 shows that our algorithm can also be affected by the
329 spectral property of the data matrix. We discuss several aspects of this difference in comparison to
330 the prior work, as well as other aspects of our algorithm below.
331

332 **$s_k(B)$ term in Theorem 1.1.** Our noise bound for σ depends not only on $O(k^{-1/4})$ but also on
333 the term $s_k(B)/\sqrt{n}$. One might wonder if this term diminishes as the number of data points n
334 increases, thereby weakening our central claim that $\sigma = O(k^{-1/4})$. However, $s_k(B)$ is a property
335 of the entire $d \times (n + 1)$ data matrix B . As n increases, the matrix itself grows, and its singular
336 values are generally expected to grow as well.
337

338 More precisely, for a data matrix B whose columns (the data points) have a reasonably constant
339 average norm, the squared Frobenius norm $\|B\|_F^2 = \sum_{i,j} B_{i,j}^2$ will grow approximately linearly
340 with n . Since the squared Frobenius norm for our rank- k matrix B is also equal to the sum of
341 its squared singular values, i.e., $\|B\|_F^2 = \sum_{i=1}^k s_i(B)^2$, this growth must be distributed among
342 the singular values. Furthermore, if the data matrix B is *well-conditioned*—meaning its singular
343 values are not pathologically distributed and the data points do not collapse onto a lower-dimensional
344 subspace—then individual singular values are expected to scale proportionally to $\|B\|_F = O(\sqrt{n})$.
345 Therefore, for well-conditioned data, the ratio $s_k(B)/\sqrt{n}$ is expected to converge to a non-zero
346 constant rather than decay to 0. An example of a well-conditioned matrix family is a random matrix
347 where each entry is sampled independently and identically from a random variable with mean 0,
348 variance 1, and finite fourth moment (Bai and Yin, 1993). They proved that for such an $m \times n$
349 matrix ($m \leq n$), the smallest singular value is almost surely $(1 - \sqrt{m/n})^2$. The assumption that
350 the data matrix is well-conditioned is standard for many real-world, high-dimensional datasets.
351

352 **Comparison to Prior Work (Abdullah et al., 2014).** Prior work, unlike our algorithm, does not
353 require any assumption on the singular values of the (latent) data matrix. However, this generality
354 comes at the cost of a much stricter noise requirement, where the noise level σ must be bounded
355 by an inverse polynomial in the ambient dimension d . By contrast, our approach introduces a de-
356 dependency on the data’s spectrum $s_k(B)$ but achieves significantly improved noise tolerance with
357 respect to the intrinsic dimension k . Our contribution is therefore most impactful in the common
358 scenario where the ambient dimension d is very high, but the data lies near a low-dimensional, well-
359 conditioned subspace (i.e., large d , small k). We believe this represents a valuable and practical
360 trade-off.
361

362 **Connection between Johnson-Lindenstrauss Lemma and Our Results.** The upper bounds of σ
363 in Theorem 1 depend on three terms. For the first term to be the smallest, our theorem requires $k =$
364 $\Omega(\ln n/\varepsilon^2)$. This term $\Omega(\ln n/\varepsilon^2)$ also appears in the standard Johnson-Lindenstrauss (JL) Lemma.
365 The JL Lemma states that a random projection of n data points from a d -dimensional ambient space
366 into a k -dimensional subspace preserves all pairwise distances up to a $(1 + \varepsilon)$ multiplicative factor.
367 The JL Lemma thus establishes the required dimensionality for an oblivious random projection to
368 preserve the geometry of n points, where $k = \Omega(\ln n/\varepsilon^2)$ is known to be the information-theoretic
369 complexity for the pairwise distance preservation problem.
370

371 Our result implies that for SVD to be an effective denoising strategy for NNS, the underlying sub-
372 space containing the true signal must itself have a complexity that scales in a JL-like manner. If k
373 were smaller than this threshold, the k -dimensional subspace would be too *simple* to robustly encode
374 the identity of the nearest neighbor against noise across all n points. In summary, the JL Lemma
375 focuses on dimensionality reduction (from $d \rightarrow k$) using random projections. Conversely, our work
376 addresses denoising when the data already possesses a low intrinsic dimension k . We demonstrate
377 that if the data has this structure and k satisfies this fundamental complexity requirement, then us-
378 ing SVD enables accurate NNS recovery in a high-noise regime ($\sigma = O(k^{-1/4})$), a regime where
379 standard JL would fail to preserve the nearest neighbor identity.
380

378 **Matrix Split Ratio Choice.** In our algorithm, we split the perturbed point set into two halves.
 379 This 50-50 split ratio is actually a minimax optimal choice. The primary goal of splitting the data
 380 is to obtain a set of learned singular vectors (e.g., spanning subspace $U^{(2)}$) that are stochastically
 381 independent of the noise in the data we intend to denoise (e.g., $A^{(1)}$). The accuracy of this learned
 382 subspace $U^{(2)}$ as an estimate for the true latent subspace V depends directly on the number of data
 383 points used to compute it (i.e. $(1 - p)n$). A smaller partition size leads to a less stable SVD and a
 384 larger error in the estimated subspace, as quantified by the bounds on $\|P_{U^{(2)}} - P_V\|$ in our proofs
 385 (Lemma 2.4). Note that the algorithm's overall performance is limited by the weaker of the two
 386 subspace estimations. Therefore, due to the inherent symmetry of our algorithm, the 50 – 50 split
 387 maximizes the size of the smaller partition, thereby providing the most robust performance when no
 388 prior information about the data's structure is known.

389 **Runtime of the Algorithm 1.** The running time of our methods just involves two SVD calculations
 390 on the two halves of the matrix, and using iterative methods, such as those in (Musco and
 391 Musco, 2015), each can be done in $O(ndk / \min(1, \sqrt{\text{gap}}))$ time, up to logarithmic factors, where
 392 $\text{gap} = s_k/s_{k+1} - 1$. For our recovery guarantees (Theorem 1.1), we require $s_k(B)$ to be suf-
 393 ficiently larger than σ . Then we expect that $s_k(A) \sim s_k(B)$ and $s_{k+1}(A) \sim \sigma$, which implies
 394 $\text{gap} = s_k(A)/s_{k+1}(A) - 1$ will be large. This helps both for recovery and for the efficiency of the
 395 SVD calculation. We then need to project the data onto the top k components we find, which is
 396 $O(ndk)$ time.

397 **Requirement to Know the Intrinsic Dimension k .** In our setting, we need to know k to run our
 398 algorithm. In other words, choosing a cutoff $k' > k$ would imply $s_{k'} = 0$, yielding a vacuous bound.
 399 However, real-world data is often full-rank with a decaying spectrum. In practice, selecting $k' > k$
 400 is a valid heuristic to capture signal "leakage" into lower singular values without capturing the bulk
 401 of the noise spectrum.

404 3 LOWER BOUNDS

406 In Theorem 1.1, we showed an algorithmic result for which $\sigma \in O(1/k^{1/4})$ (resp. $\sigma \in O(\varepsilon)$). In
 407 this section, we demonstrate that this dependence on k (resp. ε) for σ is optimal by establishing an
 408 information-theoretic lower bound showing that $\sigma = O(1/k^{1/4})$ (resp. $\sigma \in O(\varepsilon)$) is necessary. We
 409 prove this hardness result for a computationally easier problem than the one we have addressed. Let
 410 p_1, \dots, p_n, q be points in \mathbb{R}^k . We note that reducing the dimension of the ambient space only makes
 411 the problem easier in our reduction. Let $\delta_1, \dots, \delta_n, \delta_q$ be noise vectors where each component is
 412 drawn independently and identically from $N(0, \sigma^2)$. We observe the perturbed points: $\tilde{p}_i = p_i + \delta_i$,
 413 and $\tilde{q} = q + \delta_q$.

415 3.1 DEPENDENCE ON THE SUBSPACE DIMENSION k

416 The following sequence represents a reduction from the original problem to our target problem.
 417 Specifically, we are starting from our NN recovery problem and making the problem instance easier
 418 for any potential algorithm to solve. If we can prove that even this simplified, easier problem is
 419 impossible to solve reliably, it immediately implies that the original, harder problem (with the larger
 420 gap) must also be impossible to solve. We assume $\varepsilon > 0$ is a fixed constant throughout this chain of
 421 reductions and each step introduces at most a constant change in parameters.

- 423 • Given $\tilde{p}_1, \dots, \tilde{p}_n, \tilde{q}$, there is a unique index j^* such that $\|q - p_{j^*}\| \leq 1$. All other points
 424 satisfy $\|q - p_j\| \geq 1 + \varepsilon$. The goal is to output j^* .
- 425 • Given \tilde{p}_1, \tilde{p}_2 , the goal is to distinguish between the two cases: (i) $p_1 = \mathbf{0}$ and $\|p_2\| \geq 1$, or
 426 (ii) $\|p_1\| \geq 1$ and $p_2 = \mathbf{0}$.
- 427 • Given \tilde{p}_1, \tilde{p}_2 , the goal is to distinguish between the two cases: (i) $p_1 = \mathbf{0}$ and $p_2 \sim$
 428 $N(0, \frac{1}{k} I_k)$, or (ii) $p_1 \sim N(0, \frac{1}{k} I_k)$ and $p_2 = \mathbf{0}$.

430 To show the reduction from the first problem to the second, we show that the second problem is
 431 a special case of the first: Consider the case where the first problem has $n = 2$, $q = \mathbf{0}$. If $p_1 =$
 $\mathbf{0}$, $\|p_2\| \geq 1$, the only correct answer to NN is p_1 (p_2 is not a valid answer). If $\|p_1\| \geq 1$, $p_2 = \mathbf{0}$, the

432 only correct answer is 2. The final reduction step is based on the concentration of the chi-squared
433 distribution. For asymptotically large k , this concentration implies that any $p \sim N(0, \frac{1}{k}I_k)$ has a
434 norm that is almost 1 except with exponentially small probability.

435 The following lemma is a hardness result for the last problem:

436 **Lemma 3.1.** *Suppose X, Y are random vectors in \mathbb{R}^k , where $X \sim N(0, \sigma^2 I_k)$ and $Y \sim N(0, (\sigma^2 +$
437 $\frac{1}{k})I_k)$. If $\sigma \in \omega(1/k^{1/4})$, then given the unordered pair $\{X, Y\}$, no test can tell which distribution
438 the sample came from with high probability.*

440 441 3.2 DEPENDENCE ON THE DISTANCE GAP ε

442 In a similar way as in Section 3.1, we reduce the original NN recovery problem to a computationally
443 simpler one to facilitate hardness analysis. The problem reduction details are available in the
444 appendix. We only give the final lemma below:

445 **Lemma 3.2.** *Suppose X, Y are random vectors in \mathbb{R}^k , where $X \sim N(\mathbf{e}_1, \sigma^2 I_k)$ and $Y \sim N((1 +$
446 $\varepsilon)\mathbf{e}_1, \sigma^2 I_k)$. If $\sigma \in \omega(\varepsilon)$, then given the unordered pair $\{X, Y\}$, no test can tell which distribution
447 the sample came from with high probability.*

448 449 4 EXPERIMENTS

450 In this section, we implement and evaluate our main algorithm. First, we show that it empirically
451 outperforms the naïve algorithm, suggesting that the denoising effect of the SVD is significant.
452 Second, we demonstrate that our analysis in Corollary 2.8 is tight with respect to the parameter
453 $s_k(B)$.

454 455 4.1 EXPERIMENTAL EVALUATION

456 We first describe the details of our initial experiment. Our main algorithm is simple to implement.
457 As a baseline, we compare it against a naïve algorithm that selects the index minimizing $\|Ax_j\|$
458 over $1 \leq j \leq n$, where $x'_j = \mathbf{e}_{n+1} - \mathbf{e}_j$. This naïve method is affected by the ambient space \mathbb{R}^d
459 when determining the noise threshold σ required for successful recovery, while our main algorithm
460 depends only on the latent subspace dimension k (specifically, $\sigma = O(k^{-1/4})$). Note that this naïve
461 method does not mean the algorithm in the (Abdullah et al., 2014). We could not use them as a base-
462 line because their time and space complexity made implementation infeasible for our experimental
463 setup.

464 We evaluate our algorithm on two real datasets from different domains: one image-based and one
465 text-based. Throughout the experiments, we fix the parameters as follows: $n = 3\,000$, $k = 30$, and
466 $\varepsilon = 0.05$. For a given dataset and fixed noise level σ , we perform 100 queries to compute the success
467 probability. As our algorithm is efficient and simple to implement, all experiments were conducted
468 on a CPU with an M1 chip and 16 GB of RAM. We give the full details of our datasets.

469 **1) GloVe¹:** This is a set of pre-trained word embeddings where each English word is represented
470 by a high-dimensional real vector. We use the GloVe Twitter 27B dataset, which provides 1 193 514
471 word vectors of dimension 200. We randomly sample $n = 3\,000$ to construct the data matrix B .

472 **2) MNIST²:** MNIST consists of 70 000 images of handwritten digits (0-9) in grayscale, of which
473 60 000 are training and 10 000 testing. Each image is 28×28 , yielding a 784-dimensional vector of
474 pixel intensities. We sample $n = 3\,000$ training images (flattened to $d = 784$) as data points.

475 *Preprocessing.* To align the real-world datasets with our theoretical model, we first performed a
476 rank- k approximation on the data matrix B . We then selected queries and rescaled the data to
477 ensure the nearest neighbor was at distance 1 and all other points were at least $1 + \varepsilon$ away. The full
478 preprocessing details are available in the appendix.

479 *Results.* Across both datasets, our main algorithm consistently outperforms the naïve algorithm
480 across the full range of σ values. In particular, the failure threshold—the smallest σ at which NN

481 ¹<https://nlp.stanford.edu/projects/glove/>

482 ²<http://yann.lecun.com/exdb/mnist/>

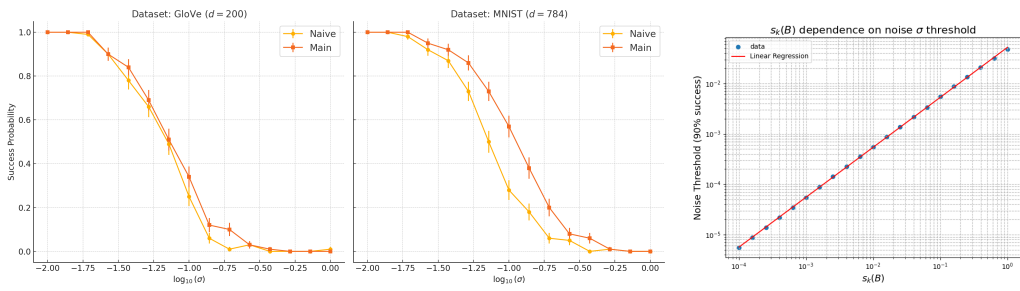


Figure 1: Performance comparison on two real-world datasets (left) and analysis of the noise threshold's dependence on the singular value $s_k(B)$ (right).

recovery becomes unreliable—is significantly higher for our algorithm. We observe two characteristic noise regimes: one where the noise is too small to affect the NN, and another where recovery is information-theoretically impossible. Between these extremes lies a meaningful intermediate regime in which the performance of the two algorithms diverges. In this regime, the performance gap is more pronounced when the ambient dimension d is large. The qualitative results are consistent across both image (MNIST) and text (GloVe) domains, indicating cross-domain robustness. These results illustrate the practical benefits of our approach.

4.2 DEPENDENCE ON $s_k(B)$

We now describe the details of our second experiment. While the analyses in Sections 2 and 3 characterize the algorithm's performance in terms of the subspace dimension k and the distance gap ε , it is also of interest to examine its dependence on $s_k(B)$. In Corollary 2.8, we showed that our algorithm exhibits a linear dependence: $\sigma = O(s_k(B))$. Our empirical results confirm these dependencies, suggesting that the analysis is tight.

Data Generation. For the second experiment, we generated synthetic data to analyze the algorithm's dependence on $s_k(B)$. We constructed the data matrix B via an SVD-based approach, allowing us to explicitly control its singular values. A subsequent procedure was used to embed a query and its nearest neighbor to satisfy the $1 + \varepsilon$ distance gap condition. A detailed description of the data generation process can be found in the appendix.

Results. In this plot, we observe a clear linear dependence on each parameter across the full range of σ . The *noise threshold* is defined as the value of σ at which the success probability first drops below 90% for a given parameter setting. For each parameter configuration, we repeat the experiment 100 times to estimate the success probability. These results demonstrate that our theoretical analysis is tight. Note that this does not imply the optimality of our algorithm with respect to $s_k(B)$.

REFERENCES

Amirali Abdullah, Alexandr Andoni, Ravindran Kannan, and Robert Krauthgamer. Spectral approaches to nearest neighbor search. *arXiv preprint arXiv:1408.0751*, 2014.

William B Johnson and Joram Lindenstrauss. Extensions of lipshitz mapping into hilbert space. *Contemporary Mathematics*, 26:189–206, 1984.

Piotr Indyk and Rajeev Motwani. Approximate nearest neighbor: towards removing the curse of dimensionality. In *Proceedings of the Symposium on Theory of Computing (STOC)*, pages 604–613, 1998.

Mayur Datar, Nicole Immorlica, Piotr Indyk, and Vahab S Mirrokni. Locality-sensitive hashing scheme based on p-stable distributions. In *Proceedings of the ACM Symposium on Computational Geometry (SoCG)*, 2004.

Alexandr Andoni and Piotr Indyk. Near-optimal hashing algorithms for approximate nearest neighbor in high dimensions. In *Proceedings of the Symposium on Foundations of Computer Science (FOCS)*, pages 459–468, 2006.

Alexandr Andoni, Piotr Indyk, Huy Nguyen, and Ilya Razenshteyn. Beyond locality-sensitive hashing. In *Proceedings of the ACM-SIAM Symposium on Discrete Algorithms (SODA)*, 2014.

540 James McNames. A fast nearest-neighbor algorithm based on a principal axis search tree. *Pattern Analysis and*
541 *Machine Intelligence, IEEE Transactions on*, 23(9):964–976, 2001.

542

543 Robert F Sproull. Refinements to nearest-neighbor searching in k-dimensional trees. *Algorithmica*, 6:579–589,
544 1991.

545

546 Nikhilesh Verma, Samy Kpotufe, and Sanjoy Dasgupta. Which spatial partition trees are adaptive to intrinsic
547 dimension? In *Proceedings of the Twenty-Fifth Conference on Uncertainty in Artificial Intelligence*, pages
548 565–574. AUAI Press, 2009.

549

550 Yair Weiss, Antonio Torralba, and Rob Fergus. Spectral hashing. In *Advances in neural information processing*
551 *systems*, pages 1753–1760, 2008.

552

553 Ruslan Salakhutdinov and Geoffrey Hinton. Semantic hashing. *International Journal of Approximate Reasoning*,
554 50(7):969–978, 2009.

555

556 National Research Council. *Frontiers in Massive Data Analysis*. The National Academies Press, 2013. Available
557 from: http://www.nap.edu/catalog.php?record_id=18374.

558

559 Noga Alon. Problems and results in extremal combinatorics i. *Discrete Mathematics*, 273:31–53, 2003.

560

561 T S Jayram and David P Woodruff. Optimal bounds for johnson-lindenstrauss transforms and streaming prob-
562 lems with subconstant error. *ACM Transactions on Algorithms*, 9(3):26, 2013. Previously in SODA’11.

563

564 Christos H Papadimitriou, Prabhakar Raghavan, Hisao Tamaki, and Santosh S Vempala. Latent semantic in-
565 dexing: A probabilistic analysis. *J. Comput. Syst. Sci.*, 61(2):217–235, 2000.

566

567 Yossi Azar, Amos Fiat, Anna Karlin, Frank Mcsherry, and Jared Saia. Spectral analysis of data. *Conference*
568 *Proceedings of the Annual ACM Symposium on Theory of Computing*, 01 2001. doi: 10.1145/380752.
380859.

569

570 Chandler Davis and W. M. Kahan. The rotation of eigenvectors by a perturbation. iii. *SIAM Journal on*
571 *Numerical Analysis*, 7(1):1–46, 1970. ISSN 00361429. URL <http://www.jstor.org/stable/2949580>.

572

573 Per-Åke Wedin. Perturbation bounds in connection with singular value decomposition. *BIT Numerical Mathe-
574 matics*, 12(1):99–111, 1972.

575

576 Sean O’Rourke, Van Vu, and Ke Wang. Random perturbation of low rank matrices: Improving classical bounds.
577 *Linear Algebra and its Applications*, 540:26–59, 2018. ISSN 0024-3795. doi: <https://doi.org/10.1016/j.laa.2017.11.014>.

578

579 Mark Rudelson and Roman Vershynin. Non-asymptotic theory of random matrices: extreme singular values.
580 In *Proceedings of the International Congress of Mathematicians 2010 (ICM 2010) (In 4 Volumes) Vol. I:
581 Plenary Lectures and Ceremonies Vols. II–IV: Invited Lectures*, pages 1576–1602. World Scientific, 2010.

582

583 Z. D. Bai and Y. Q. Yin. Limit of the smallest eigenvalue of a large dimensional sample covariance matrix. *The*
584 *Annals of Probability*, 21(3):1275–1294, 1993. ISSN 00911798, 2168894X. URL <http://www.jstor.org/stable/2244575>.

586

587 Cameron Musco and Christopher Musco. Randomized block krylov methods for stronger and faster approxi-
588 mate singular value decomposition. *Advances in neural information processing systems*, 28, 2015.

589

590 B. Laurent and P. Massart. Adaptive estimation of a quadratic functional by model selection. *The Annals of*
591 *Statistics*, 28(5):1302 – 1338, 2000. doi: 10.1214/aos/1015957395.

592

593 Luc Devroye, Abbas Mehrabian, and Tommy Reddad. The total variation distance between high-dimensional
gaussians with the same mean. *arXiv preprint arXiv:1810.08693*, 2023.

594 **A SUPPLEMENTARY MATERIAL**

595 **A.1 POSTPONED PROOFS**

598 **A.1.1 PROOF OF LEMMA 2.4**

599 *Proof.* $B^{(1)}$'s columns all lie in V . So, $s_{k+1}(B^{(1)}) = 0$. Thus, instantiating Lemma 2.2 gives:

601
$$\|P_{U^{(2)}} - P_V\| \leq \frac{2\|C^{(2)}\|}{s_k(B^{(2)})}. \quad (3)$$

604 Note that $C^{(2)}$ is a $d \times (\frac{n}{2} + 1)$ matrix. Applying Lemma 2.3 with $t = \sigma\sqrt{2\ln(8n^2)}$ gives:

606
$$\|P_{U^{(2)}} - P_V\| \leq \frac{2\|C^{(2)}\|}{s_k(B^{(2)})} \leq \frac{2\sigma}{s_k(B^{(2)})} \left(\sqrt{d} + \sqrt{\frac{n}{2} + 1} + \sqrt{2\ln(8n^2)} \right) \leq \frac{8\sigma\sqrt{n}}{s_k(B^{(2)})} \quad (4)$$

608 with at least $1 - \frac{1}{4n^2}$ probability (using $n \geq d, 10$). In conclusion, the lemma is proved as follows:

610
$$\Pr \left[\left\| (P_{U^{(2)}} - P_V)B^{(1)}x_j \right\|^2 \leq \frac{100\sigma^2 n}{s_k^2(B^{(2)})} \left\| B^{(1)}x_j \right\|^2 \right] \geq 1 - \frac{1}{4n^2}$$

612 for all $1 \leq j \leq n/2$. □

613 **A.1.2 PROOF OF LEMMA 2.5**

615 *Proof.* From the definition of $C^{(1)}$ and x_j , the vector $y := C^{(1)}x_j \in \mathbb{R}^d$ is just a summation of two
616 Gaussian random vectors. Thus, $y \sim N(0, 2\sigma^2 I_d)$. Also, for any basis $\{u_1, \dots, u_k\}$ of $\text{col}(U^{(2)})$,
617 since $P_{U^{(2)}}$ is a projection matrix, the following holds:

619
$$\left\| P_{U^{(2)}} C^{(1)}x_j \right\|^2 = \sum_{i=1}^k (u_i^T y)^2.$$

622 Note that $P_{U^{(2)}}$ and $C^{(1)}$ are stochastically independent (since P_{shU} depends only on $C^{(2)}$ and not
623 on $C^{(1)}$). Since $y \sim N(0, 2\sigma^2 I_d)$ is spherically symmetric, its entries $X_i = u_i^T y$ are independent
624 $N(0, 2\sigma^2)$ random variables. Hence

626
$$\sum_{i=1}^k (u_i^T y)^2 = \|X\|^2 = 2\sigma^2 \cdot \sum_{i=1}^k \left(\frac{X_i}{\sqrt{2\sigma^2}} \right)^2 = 2\sigma^2 Z$$

628 where $Z \sim \chi_k^2$. Now we can apply the Laurent–Massart tail bound (Laurent and Massart, 2000) for
629 χ^2 distribution.

630
$$\forall x \geq 0, \Pr \left[|Z - k| > 2\sqrt{kx} + 2x \right] \leq e^{-x}.$$

632 Setting $x = 6\ln n$, using the Laurant–Massart bound and taking the union over $j = 1, 2, 3 \dots n/2$
633 gives us the Lemma. □

634 **A.1.3 PROOF OF LEMMA 2.6**

636 *Proof.* We have

638
$$\left\| B^{(1)T} x_j^T (P_{U^{(2)}} - P_V) B^{(1)} x_j \right\| \leq \|P_{U^{(2)}} - P_V\| \left\| B^{(1)} x_j \right\|^2. \quad (5)$$

639 Applying (4) to the right hand side, the proof completes. □

641 **A.1.4 PROOF OF LEMMA 2.7**

643 *Proof.* Let $y := x_j^T B^{(1)T} P_{U^{(2)}}$. y and $C^{(1)}x_j$ are stochastically independent (Recall that B is not
644 random, but, a fixed matrix.) So, $y C^{(1)}x_j$ is a real-valued Gaussian random variable with distribution
645 $N(0, 2\|y\|^2 \sigma^2)$. Further, $\|y\| \leq \|B^{(1)}x_j\|$ since $P_{U^{(2)}}$ is a projection matrix. Now, the Lemma
646 follows by standard Gaussian tail bounds.

647

□

648 A.1.5 PROOF OF LEMMA 3.1
649

650 *Proof.* We want to calculate the KL divergence between two distributions. Let $P_1 = N(0, \sigma^2 I_k)$
651 and $P_2 = N(0, (\sigma^2 + \frac{1}{k}) I_k)$. We evaluate this by computing the KL divergence between the joint
652 distributions $R_1(x, y) = P_1(x)P_2(y)$ and $R_2(x, y) = P_2(x)P_1(y)$. Note that these two distributions
653 differ only by a swap. Since the KL divergence is additive for independent distributions, the
654 following holds:

$$655 \quad D_{KL}(R_1||R_2) = D_{KL}(P_1||P_2) + D_{KL}(P_2||P_1).$$

656 The formula for the KL divergence between two multivariate k -dimensional gaussian distributions
657 $Q_1 = N(\mu_1, \Sigma_1)$ and $Q_2 = N(\mu_2, \Sigma_2)$ is:

$$659 \quad D_{KL}(Q_1||Q_2) = \frac{1}{2} \left[\log \frac{|\Sigma_2|}{|\Sigma_1|} - k + \text{tr}\{\Sigma_2^{-1}\Sigma_1\} + (\mu_2 - \mu_1)^T \Sigma_2^{-1}(\mu_2 - \mu_1) \right].$$

662 Using the above formula, we get
663

$$664 \quad 2D_{KL}(R_1||R_2) = k \log \frac{\sigma^2 + (1/k)}{\sigma^2} - k + k \frac{\sigma^2}{\sigma^2 + (1/k)} \\ 665 \quad + k \log \frac{\sigma^2}{\sigma^2 + (1/k)} - k + k(1 + (1/k\sigma^2)) \\ 666 \quad = -2k + k \frac{1}{1 + (1/k\sigma^2)} + k + \frac{1}{\sigma^2} \leq \frac{1}{k\sigma^4},$$

671 using $1/(1 + \eta) \leq 1 - \eta + \eta^2$ for $\eta \in [0, 1]$. Therefore, the KL divergence approaches 0 when
672 $\sigma = \omega(k^{-1/4})$. This means that it becomes impossible to determine which distribution the observed
673 vector came from as k grows large. \square
674

675 A.1.6 PROOF OF LEMMA 3.2
676

677 *Proof.* Translating both distributions by $-\mathbf{e}_1$ and scaling by $1/\sigma$ reduces the problem to distinguishing
678 $N(0, I_k)$ from $N((\varepsilon/\sigma)\mathbf{e}_1, I_k)$ while preserving distinguishability. Because the coordinates are
679 independent and identical except for the mean shift in the first coordinate, the optimal test depends
680 only on the first coordinate. Thus, the task is equivalent to distinguishing the 1-dimensional Gaussian
681 distribution $N(0, 1^2)$ and $N(\varepsilon/\sigma, 1^2)$. According to (Devroye et al., 2023), the total variation
682 distance between two one-dimensional Gaussian distributions with unit variance is at most half the
683 difference of their means. Therefore, $d_{TV}(N(0, 1^2), N(\frac{\varepsilon}{\sigma}, 1^2)) \leq \frac{\varepsilon}{2\sigma}$, which implies that based
684 on the observed vector, it becomes impossible to determine which distribution it came from as
685 $\frac{\varepsilon}{\sigma} \rightarrow 0$. \square
686

687 A.2 POSTPONED DETAILS
688

689 A.2.1 COMPARISON OF NOISE TOLERANCE REGIMES
690

Noise Regime	Magnitude	Random Projection	Abdullah et al. (2014)	SVD (Ours)
$\sigma \ll 1/\sqrt{d}$	$o(1)$	✓ Succeeds	✓ Succeeds	✓ Succeeds
$\sigma \in O(1/d^{1/4})$	$\approx \sigma\sqrt{d}$	✗ Fails	✓ Succeeds	✓ Succeeds
$\sigma \in O(1/k^{1/4})$	$\approx \sigma\sqrt{d}$	✗ Fails	✗ Fails	✓ Succeeds
$\sigma \gg 1/k^{1/4}$	$\approx \sigma\sqrt{d}$	✗ Fails	✗ Fails	✗ Fails (info-theoretic)

699 Table 1: Comparison of Noise Tolerance Regimes. SVD succeeds in the “Intermediate” regime
700 where the noise norm is large enough to break Random Projections (RP), but structured enough to
701 be filtered by SVD.

702 A.2.2 PROBLEM REDUCTION DETAILS FOR SECTION 3.2
703

704 The following describes the original problem and the simplified target problem:

705 • Given $\tilde{p}_1, \dots, \tilde{p}_n, \tilde{q}$, there is a unique index j^* such that $\|q - p_{j^*}\| \leq 1$. All other points
706 satisfy $\|q - p_j\| \geq 1 + \epsilon$. The goal is to output j^* .
707

708 • ($n = 2$ and $q = \mathbf{0}$) Given \tilde{p}_1, \tilde{p}_2 , there is a unique index j^* such that $\|p_{j^*}\| \leq 1$. The other
709 point satisfies $\|p_j\| \geq 1 + \epsilon$. The goal is to output j^* .
710

711 • (Fix the data generation process) Given \tilde{p}_1, \tilde{p}_2 , distinguish between the two cases: (i) $p_1 =$
712 \mathbf{e}_1 and $p_2 = (1 + \epsilon)\mathbf{e}_1$, or (ii) $p_1 = (1 + \epsilon)\mathbf{e}_1$ and $p_2 = \mathbf{e}_1$.

713 A.2.3 PREPROCESSING DETAILS FOR SECTION 4.1

714 Our theoretical guarantees assume that the data lies entirely in a k -dimensional subspace, which
715 does not strictly hold in real datasets. However, both datasets exhibit low intrinsic dimensionality,
716 as indicated by the decay of their singular values. To align with the theoretical assumptions and
717 highlight performance within a low-rank subspace, we apply a rank- k approximation to the sampled
718 matrix B by retaining only its top k singular components. This transformation preserves the essential
719 structure of the data while making the setup consistent with our analysis.

720 For each dataset, we generate 100 *query points* by projecting held-out data onto the rank- k subspace
721 and selecting points whose nearest-to-second-nearest neighbor distance ratio is just above $1 + \epsilon$. Due
722 to the dataset structure, all GloVe vectors are eligible as query candidates, while for MNIST, queries
723 are sampled from the test set. After that, each column is rescaled such that the NN lies exactly at
724 distance 1 from the query point, and i.i.d. noise $N(0, \sigma^2)$ is added. Finally, we randomly shuffle the
725 first n columns to ensure that both $B^{(1)}$ and $B^{(2)}$ have rank k , as required by Theorem 1.1.

726 A.2.4 DATA GENERATION DETAILS FOR SECTION 4.2

727 Unlike in the first experiment, this experiment is conducted on randomly generated datasets. The
728 purpose here is to find concrete examples that clearly reveal the linear dependence of our algorithm
729 on $s_k(B)$. We fix the parameters as follows: $n = 200$, $d = 100$, $k = 10$, and $\epsilon = 0.05$. To study
730 the dependence on $s_k(B)$, we start with the SVD decomposition $B = X\Sigma Y^\top$, where X and Y are
731 orthogonal matrices randomly generated via QR decomposition of random Gaussian matrices. The
732 singular values of B are controlled by setting the diagonal entries of Σ .
733

734 However, the resulting matrix $B = X\Sigma Y^\top$ may not automatically satisfy the distance gap condition—that is, the requirement that the NN lies at distance exactly 1 from the query point, and the
735 second NN is at distance at least $1 + \epsilon$. To enforce this condition, we proceed as follows. We first
736 generate the first $n - 1$ columns of B using the above procedure.
737

738 Then, we sample a random direction \vec{u} that lies in the intrinsic k -dimensional subspace V . Essentially,
739 we embed the query point $q = t_1\vec{u}$ and the n -th point $p_n = t_2\vec{u}$ in the space for some scalars
740 t_1 and t_2 . The value t_1 is set by starting from $+\infty$ and decreasing it until the distance between the
741 nearest neighbor among the other $n - 1$ points and $t_1\vec{u}$ becomes $1 + \epsilon$. Then, we set $t_2 = t_1 + 1/\|\vec{u}\|$,
742 which makes the distance between the query point and this n -th point exactly 1. This construction
743 makes the query point, its nearest neighbor, and the origin collinear. While one could add noise to
744 these points to avoid this artificial collinearity, we believe it would not affect the performance of the
745 algorithms in our context.
746

747
748
749
750
751
752
753
754
755